Nearside−Farside Analysis of Differential Cross Sections: Ar + HF Rotationally Inelastic Scattering†

T. W. J. Whiteley,‡ C. Noli, and J. N. L. Connor*

Department of Chemistry, University of Manchester, Manchester M13 9PL, United Kingdom

Received: January 3, 2001; In Final Form: January 18, 2001

We report accurate coupled-channel quantum calculations of state-to-state and degeneracy-averaged differential cross sections for the rotationally inelastic collision Ar + HF($v_i = 0$, $j_i = 0$, $m_i = 0$) → Ar + HF($v_f = 0$, j_f, m_f), where v_i, j_i, m_i and v_f, j_f, m_f are initial and final vibrational, rotational, and helicity quantum numbers, respectively. The calculations have been performed at eight collision energies and assume that HF is a rigid rotator. Structure in the differential cross sections is analyzed using the unrestricted version of nearside−farside (NF) theory. The NF theory decomposes the partial wave series (PWS) for the helicity scattering amplitude into two subamplitudes, one N, the other F. This is the first application of NF theory to an atom-heteronuclear molecule inelastic collision. It is demonstrated that the NF technique provides a clear physical interpretation of the angular scattering, except sometimes for scattering angles, θ, close to 0° and 180°. It is also shown that a resummation of the PWS can improve the usefulness of the NF technique, when the N and F cross sections possess small oscillations. The resummation procedure exploits recurrence properties of reduced rotation matrix elements to extract a factor $(\alpha + \beta\cos\theta)^{-1}$ from the PWS, where α and β are constants. Criteria for choosing α and β so as to obtain a physically meaningful NF decomposition are discussed.

1. Introduction

The scattering of HF by Ar is an important example of rotational energy transfer for the collision of a heteronuclear diatomic molecule with an atom. State-to-state integral cross sections (for vibrationally excited HF) have been measured by Barnes et al.,[1,2] while experimental angular distributions have been reported by Vohralik et al.,[3] Rawluk et al.,[4] and Chapman et al.[5] for the vibrational ground state of HF. There have also been many spectroscopic studies of the ArHF van der Waals complex. Hutson[6] has used the spectroscopic data to construct an intermolecular potential energy function that has performed well in reproducing[5,7−9] the scattering measurements (see also refs 10−13).

The purpose of this paper is to report a theoretical investigation of the angular scattering for the collision

$$\mathrm{Ar} + \mathrm{HF}(v_i = 0, j_i = 0, m_i = 0) \rightarrow \mathrm{Ar} + \mathrm{HF}(v_f = 0, j_f, m_f) \quad (1.1)$$

where v_i, j_i, m_i and v_f, j_f, m_f are vibrational, rotational, and helicity quantum numbers for the initial and final states, respectively. The helicities m_i, m_f are the quantum numbers associated with the projection of the HF rotational angular momentum onto the relative velocity vector. Our calculations have been stimulated by pevious theoretical research, in particular that of Rawluk et al.[7] and of Barrett et al.[8,9] Their work has shown that the degeneracy-averaged differential cross sections for HF + Ar exhibit interesting structures, which depend on the balance between the attractive and repulsive anisotropies in the intermolecular potential.

This paper makes three contributions to understanding the dynamics of the HF + Ar collision system:

(1) We report accurate quantum coupled-channel (CC) scattering calculations of state-to-state and degeneracy averaged angular distributions using the Hutson potential assuming that HF is a rigid rotator. These calculations, which extend earlier work,[5,7−9] have been performed at eight collision energies, with the lowest one being that used in the dopplerimetry experiment of Chapman et al.,[5] while the highest one is that employed in the crossed molecular beam experiment of Rawluk et al.[4]

(2) We carry out *nearside−farside* (NF) analyses of the CC angular distributions obtained in (1). This is the first application of NF theory[14−25] to the differential cross sections of heteronuclear-molecule atom collisions.

It is well-known that CC computations have the disadvantage that it is difficult (and often impossible) to understand the physical origin of structure in the angular scattering.[26] This is because many numerically significant terms contribute to the partial wave series (PWS) representation of the scattering amplitude. Recently, however, it has been shown that the NF method[14−25] provides a relatively simple way to extract (partial) physical information from a CC computation of the PWS.

In a NF analysis, the PWS scattering amplitude is decomposed into two subamplitudes. These are the N subamplitude, which is associated with semiclassical trajectories scattered from the nearside of the target, and the F subamplitude, which is associated with semiclassical trajectories scattered from the farside of the target. Structure in an angular distribution can arise from the N subamplitude, or from the F subamplitude or from interference between the N and F subamplitudes. It is important to note that the inputs to a NF analysis are the same CC scattering matrix elements that are used to sum the PWS for the full scattering amplitude. Also semiclassical techniques, such as saddle point or stationary phase integration are not used, although the semiclassical picture is still evident.

† Part of the special issue "William H. Miller Festschrift".

‡ Present address: Micromass UK Ltd., Floats Rd., Wythenshaw, Manchester M23 9LZ, United Kingdom.

10.1021/jp0100046 CCC: $20.00
Published on Web 02/28/2001

(3) We apply *resummation* techniques[22,23] to the PWS for the scattering amplitude. In particular, we show that a resummation of the PWS followed by a NF decomposition provides a clear physical interpretation of the angular scattering for those cases where the N and F cross sections for the unresummed PWS possess unphysical oscillations. The resummation exploits recurrence properties of reduced rotation matrix elements.

In all three applications just described, the initial and final vibrational quantum numbers for HF are kept fixed at $v_i = v_f = 0$. The labels v_i, v_f will therefore be omitted from now on, to keep the notation as simple as possible. The NF theory for collision (eq 1.1) is presented in section 2, while section 3 describes the resummation of the PWS. The intermolecular potential and CC computations are outlined in section 4. Our CC and NF results for the angular scattering are presented and discussed in section 5. Section 6 contains our conclusions.

2. Nearside−Farside Analysis

Nearside−farside theory has been used to analyze the differential cross sections of many different elastic and inelastic collision systems:[17,20,25] He + Ne, H^+ + Ar, Ne + D_2, He + N_2, and Ar + N_2 as well as the reactions[14−16,18,24] Cl + HCl → ClH + Cl, F + H_2 → FH + H, F + HD→ FH + D (or FD + H), and H + D_2 → HD + D. This Section presents the key equations[17,25] needed to carry out a NF analysis for the differential cross section of a general state-to-state A + BC inelastic collision.

The starting point is the PWS for the scattering amplitude, $f_{j_f m_f \leftarrow j_i m_i}(\theta)$, in the helicity representation:[27, 28]

$$f_{j_f m_f \leftarrow j_i m_i}(\theta) = (2ik_{j_i})^{-1} \sum_{J=J_{\min}}^{\infty} (2J+1)(S^J_{j_f m_f \leftarrow j_i m_i} - \delta_{j_f j_i}\delta_{m_f m_i}) d^J_{m_f,m_i}(\theta) \quad (2.1)$$

where θ is the scattering angle, k_{j_i} is the translational wavenumber for relative motion in the initial channel, J is the total angular momentum quantum number, $S^J_{j_f m_f \leftarrow j_i m_i}$ is a *body-fixed* scattering matrix element, $\delta_{j_f j_i}$ is a Kronecker delta function and $d^J_{m_f,m_i}(\theta)$ is a reduced rotation matrix element as defined by Edmonds.[29] A constant phase has been omitted when writing down eq 2.1. The state-to-state differential cross section is given by

$$I_{j_f m_f \leftarrow j_i m_i}(\theta) = |f_{j_f m_f \leftarrow j_i m_i}(\theta)|^2 \quad (2.2)$$

Possible values for m_f, m_i in eq 2.1 are 0, ±1, ±2, ..., ±J with J = 0, 1, 2, ... The first nonzero term occurs for $J = J_{\min} = \max(|m_f|,|m_i|)$. It is convenient in the NF analysis[17,25] to use values for m_f, m_i such that $m_f - m_i$ and $m_f + m_i$ are always ≥ 0, i.e., we require $J \geq m_f \geq |m_i|$. This can be achieved by means of the following symmetry relations obeyed by the $d^J_{m_f,m_i}(\theta)$ [ref 29, p 60, eqs 4.2.5 and 4.2.6]

$$d^J_{m_f,m_i}(\theta) = (-1)^{m_f - m_i} d^J_{m_i,m_f}(\theta) = (-1)^{m_f - m_i} d^J_{-m_f,-m_i}(\theta) = d^J_{-m_i,-m_f}(\theta) \quad (2.3)$$

In the following, we shall assume that this ordering of m_f and m_i has been done. It then follows that $J_{\min} = m_f \geq 0$.

Our aim is to separate the scattering amplitude into two subamplitudes, N and F, corresponding to angular waves travelling clockwise and anticlockwise in θ respectively.[17,25] This can be accomplished by decomposing $d^J_{m_f,m_i}(\theta)$ into the sum of two *travelling angular functions* (for $\theta \neq 0, \pi$)

$$d^J_{m_f,m_i}(\theta) = d^{J(+)}_{m_f,m_i}(\theta) + d^{J(-)}_{m_f,m_i}(\theta) \quad (2.4)$$

where[25]

$$d^{J(\pm)}_{m_f,m_i}(\theta) = \frac{1}{2}\left[d^J_{m_f,m_i}(\theta) \mp \left(\frac{2i}{\pi}\right) e^J_{m_f,m_i}(\theta)\right] \quad (2.5)$$

In eq 2.5, $e^J_{m_f,m_i}(\theta)$ is a *reduced rotation matrix element of the second kind*. It is defined by[25]

$$e^J_{m_f,m_i}(\theta) = e^{i\pi\alpha} N^J_{m_f,m_i} [\sin(\theta/2)]^{\alpha} [\cos(\theta/2)]^{\beta} \mathbf{Q}^{(\alpha,\beta)}_{J-m_f}(\cos\theta), \quad \alpha = m_f - m_i, \quad \beta = m_f + m_i \quad (2.6)$$

where $\mathbf{Q}^{(\alpha,\beta)}_n(\cos\theta)$ is *a Jacobi function of the second kind of degree n with parameters* α *and* β defined "on the cut " $-1 < \cos\theta < 1$. The normalization factor in eq 2.6 is

$$N^J_{m_f,m_i} = \left[\frac{(J+m_f)!(J-m_f)!}{(J+m_i)!(J-m_i)!}\right]^{1/2}$$

The properties of $e^J_{m_f,m_i}(\theta)$ and $\mathbf{Q}^{(\alpha,\beta)}_n(\cos\theta)$ have been discussed in detail in refs 17, 19, and 25. In particular, $e^J_{m_f,m_i}(\theta)$ obeys the same symmetry relations (eq 2.3) as $d^J_{m_f,m_i}(\theta)$.

In the limit of large $J \gg m_f$, m_i, the following asymptotic approximations are valid[21,25] for $0 < \theta < \pi$:

$$d^J_{m_f,m_i}(\theta) \sim \left[\frac{2}{\pi\left(J+\frac{1}{2}\right)\sin\theta}\right]^{1/2} \cos\left[\left(J+\frac{1}{2}\right)\theta + \frac{1}{2}\pi(m_i - m_f) - \frac{1}{4}\pi\right] \quad (2.7)$$

and

$$e^J_{m_f,m_i}(\theta) \sim -\left[\frac{\pi}{2\left(J+\frac{1}{2}\right)\sin\theta}\right]^{1/2} \sin\left[\left(J+\frac{1}{2}\right)\theta + \frac{1}{2}\pi(m_i - m_f) - \frac{1}{4}\pi\right] \quad (2.8)$$

It then follows from eqs 2.5, 2.7, and 2.8 that

$$d^{J(\pm)}_{m_f,m_i}(\theta) \sim \left[\frac{1}{2\pi\left(J+\frac{1}{2}\right)\sin\theta}\right]^{1/2} \exp\left\{\pm i\left[\left(J+\frac{1}{2}\right)\theta + \frac{1}{2}\pi(m_i - m_f) - \frac{1}{4}\pi\right]\right\} \quad (2.9)$$

which is valid for $J \to \infty$ and $0 < \theta < \pi$. The term $\exp\{+ i[(J+\frac{1}{2})\theta]\}$ in eq 2.9 physically represents a travelling angular wave moving anticlockwise in θ. A semiclassical analysis shows that this wave typically originates from the farside of the target for an observer in the upper half of the scattering plane at infinity.[21] Conversely, the term $\exp\{- i[(J+\frac{1}{2})\theta]\}$ in eq 2.9 represents a travelling angular wave moving clockwise in θ, which typically originates semiclassically from the nearside of the target for an observer in the upper half of the scattering plane at infinity.[21] This analysis lets us identify the superscript (+) with F and the superscript (−) with N.

Substituting eq 2.4 into the PWS (eq 2.1) enables us to separate the scattering amplitude into N and F subamplitudes

$$f_{j_f m_f \leftarrow j_i m_i}(\theta) = f^{(+)}_{j_f m_f \leftarrow j_i m_i}(\theta) + f^{(-)}_{j_f m_f \leftarrow j_i m_i}(\theta) \qquad (2.10)$$

where the two subamplitudes are given by the coherent partial wave sums

$$f^{(\pm)}_{j_f m_f \leftarrow j_i m_i}(\theta) = (2ik_{j_i})^{-1} \sum_{J=J_{\min}}^{\infty} (2J+1)(S^J_{j_f m_f \leftarrow j_i m_i} - \delta_{j_f j_i}\delta_{m_f m_i}) d^{J(\pm)}_{m_f,m_i}(\theta) \qquad (2.11)$$

Using the asymptotic approximations (eq 2.9), we can see that N scattering is represented by $f^{(-)}_{j_f m_f \leftarrow j_i m_i}(\theta)$ and F scattering by $f^{(+)}_{j_f m_f \leftarrow j_i m_i}(\theta)$. The corresponding state-to-state N and F differential cross sections are given by

$$I^{(\pm)}_{j_f m_f \leftarrow j_i m_i}(\theta) = |f^{(\pm)}_{j_f m_f \leftarrow j_i m_i}(\theta)|^2 \qquad (2.12)$$

Structure in the full differential cross section

$$I_{j_f m_f \leftarrow j_i m_i}(\theta) = |f^{(+)}_{j_f m_f \leftarrow j_i m_i}(\theta) + f^{(-)}_{j_f m_f \leftarrow j_i m_i}(\theta)|^2$$

can arise from the N subamplitude, or from the F subamplitude, or from interference between the N and F subamplitudes. This NF interpretation of the angular scattering is analogous to that used to explain the diffraction pattern in the well-known two-slit experiment.[16] Typically, N scattering samples mainly the repulsive core of the intermolecular potential, while F scattering samples mainly the longer-range attractive parts of the potential.

The NF theory presented above is an example of an *unrestricted* NF decomposition.[17] *Restricted* NF decompositions, which take into account the caustics associated with $d^J_{m_f,m_i}(\theta)$ and $e^J_{m_f,m_i}(\theta)$, are developed in refs 20, 24, and 25. However, these more sophisticated NF theories will not be needed in the present paper.

In the HF + Ar applications discussed in section 5, we always have $m_i = 0$. For this special case, the following identities are valid[25]

$$d^J_{m_f,0}(\theta) = \left[\frac{(J-m_f)!}{(J+m_f)!}\right]^{1/2} P^{m_f}_J(\cos\theta) \qquad (2.13)$$

and

$$e^J_{m_f,0}(\theta) = \left[\frac{(J-m_f)!}{(J+m_f)!}\right]^{1/2} Q^{m_f}_J(\cos\theta) \qquad (2.14)$$

where $P^{m_f}_J(\cos\theta)$ and $Q^{m_f}_J(\cos\theta)$ are Ferrers' associated Legendre functions of the first and second kinds (of degree J and order m_f), respectively,[30] i.e.,

$$R^m_J(x) = (1-x^2)^{m/2}\frac{d^m R_J(x)}{dx^m}, \quad R = P, Q, \quad x = \cos\theta, \quad m = 0, 1, 2, ..., J \qquad (2.15)$$

In eq 2.15, $P_J(\cos\theta)$ is a Legendre polynomial of degree J and $Q_J(\cos\theta)$ is a Legendre function of the second kind of degree J. Equations 2.13 and 2.14 show that the NF theory can be developed in terms of associated Legendre functions when $m_i = 0$, rather than reduced rotation matrix elements.[20]

When $m_f = 0$ and $m_i = 0$, we have the further simplifications

$$d^J_{0,0}(\theta) = P_J(\cos\theta)$$

and

$$e^J_{0,0}(\theta) = Q_J(\cos\theta)$$

so the NF theory reduces to that for a Legendre PWS in this case.[14-18,22,23]

The low J terms in the PWS (eq 2.1) are usually the least semiclassical like. When they are numerically significant, their presence can lead to the failure of the NF method to provide a physically meaningful interpretation of structure in a differential cross section, e.g., both $I^{(+)}_{j_f m_f \leftarrow j_i m_i}(\theta)$ and $I^{(-)}_{j_f m_f \leftarrow j_i m_i}(\theta)$ may be very much larger than $I_{j_f m_f \leftarrow j_i m_i}(\theta)$ over a range of θ. In this situation, a resummation[22,23] of the PWS (eq 2.1), before making the NF decomposition, may provide the sought physical insight. This is discussed in the next section.

3. Resummation of Partial Wave Series

This section shows how to resum the PWS (eq 2.1). We then apply the NF decomposition of section 2 to the resummed PWS. As before, we assume $J \geq m_f \geq |m_i|$, so that $J_{\min} = m_f$. We start by writing the PWS (eq 2.1) in the more compact form

$$2ik_{j_i} f_{j_f m_f \leftarrow j_i m_i}(\theta) = \sum_{J=m_f}^{\infty} a_J d^J_{m_f,m_i}(\theta) \qquad (3.1)$$

where

$$a_J \equiv a^J_{j_f m_f \leftarrow j_i m_i} = (2J+1)(S^J_{j_f m_f \leftarrow j_i m_i} - \delta_{j_f j_i}\delta_{m_f m_i}) \qquad (3.2)$$

Next we multiply both sides of eq 3.1 by the factor $\alpha + \beta(\cos\theta) \neq 0$ where α, β are constants. In general, α, β can be complex valued, although in all our applications in section 5, the α, β are real. This results in

$$2ik_{j_i}(\alpha + \beta\cos\theta) f_{j_f m_f \leftarrow j_i m_i}(\theta) = \alpha \sum_{J=m_f}^{\infty} a_J d^J_{m_f,m_i}(\theta) + \beta \sum_{J=m_f}^{\infty} a_J \cos\theta\, d^J_{m_f,m_i}(\theta) \qquad (3.3)$$

A recurrence relation obeyed by the reduced rotation matrix elements is[25,31]

$$\cos\theta\, d^J_{m_f,m_i}(\theta) = \frac{g^J_{m_f,m_i}}{J(2J+1)} d^{J-1}_{m_f,m_i}(\theta) + \frac{m_f m_i}{J(J+1)} d^J_{m_f,m_i}(\theta) + \frac{g^{J+1}_{m_f,m_i}}{(J+1)(2J+1)} d^{J+1}_{m_f,m_i}(\theta), \quad J = m_f, m_f+1, m_f+2, ... \qquad (3.4)$$

where

$$g^{J+p}_{m_f,m_i} = [(J-m_f+p)(J+m_f+p)(J-m_i+p) \times (J+m_i+p)]^{1/2} \qquad p = 0,1 \qquad (3.5)$$

It is important to emphasize for the following derivation that the recurrence (eq 3.4) is valid for $J = m_f$ as well as for $J = m_f + 1, m_f + 2, ...$ (this statement is proved in the Appendix). When $J = m_f$, note that $d^{J-1}_{m_f,m_i}(\theta)$ is nonphysical and we set $d^{m_f-1}_{m_f,m_i}(\theta) \equiv 0$. Also eq 3.5 shows that $g^{m_f}_{m_f,m_i} = 0$ when $J = m_f$.

For the special case of $m_f = m_i = 0$ and $J = 0$, a direct substitution of these values into eq 3.4 produces the indeterminate forms 0/0. We can avoid this by first substituting $m_f = m_i = 0$ into eq 3.4, then taking the limit $J \rightarrow 0$. This results in the standard recurrence relation for Legendre polynomials because $d^J_{0,0}(\theta) = P_J(\cos\theta)$. The same limiting procedure should also be applied to some of the following equations in the special case $J = m_f = m_i = 0$.

Substituting eq 3.4 into eq 3.3 gives

$$2ik_{j_i}(\alpha + \beta\cos\theta) f_{j_f m_f \leftarrow j_i m_i}(\theta) = \beta \sum_{J=m_f}^{\infty} \frac{g^J_{m_f,m_i}}{J(2J+1)} a_J d^{J-1}_{m_f,m_i}(\theta) + \sum_{J=m_f}^{\infty} \left[\alpha + \beta \frac{m_f m_i}{J(J+1)}\right] a_J d^J_{m_f,m_i}(\theta) + \beta \sum_{J=m_f}^{\infty} \frac{g^{J+1}_{m_f,m_i}}{(J+1)(2J+1)} a_J d^{J+1}_{m_f,m_i}(\theta) \quad (3.6)$$

We next manipulate the first series on the right-hand side of eq 3.6, noting that its first term is zero

$$\beta \sum_{J=m_f}^{\infty} \frac{g^J_{m_f,m_i}}{J(2J+1)} a_J d^{J-1}_{m_f,m_i}(\theta)$$

$$= \beta \sum_{J=m_f+1}^{\infty} \frac{g^J_{m_f,m_i}}{J(2J+1)} a_J d^{J-1}_{m_f,m_i}(\theta), \quad \text{since } g^J_{m_f,m_i} d^{J-1}_{m_f,m_i}(\theta) = 0 \text{ for } J = m_f$$

$$= \beta \sum_{J=m_f}^{\infty} \frac{g^{J+1}_{m_f,m_i}}{(J+1)(2J+3)} a_{J+1} d^J_{m_f,m_i}(\theta), \quad \text{after replacing } J-1 \text{ by } J' \text{ and } J' \rightarrow J \quad (3.7)$$

In a similar way, we manipulate the third series on the right-hand side of eq 3.6

$$\beta \sum_{J=m_f}^{\infty} \frac{g^{J+1}_{m_f,m_i}}{(J+1)(2J+1)} a_J d^{J+1}_{m_f,m_i}(\theta)$$

$$= \beta \sum_{J=m_f-1}^{\infty} \frac{g^{J+1}_{m_f,m_i}}{(J+1)(2J+1)} a_J d^{J+1}_{m_f,m_i}(\theta), \quad \text{since } g^{J+1}_{m_f,m_i} d^{J+1}_{m_f,m_i}(\theta) = 0 \text{ for } J = m_f - 1$$

$$= \beta \sum_{J=m_f}^{\infty} \frac{g^J_{m_f,m_i}}{J(2J-1)} a_{J-1} d^J_{m_f,m_i}(\theta), \quad \text{after replacing } J+1 \text{ by } J' \text{ and } J' \rightarrow J \quad (3.8)$$

Substituting eqs 3.7 and 3.8 into eq 3.6 enables us to write for $\alpha + \beta\cos\theta \neq 0$

$$2ik_{j_i} f_{j_f m_f \leftarrow j_i m_i}(\theta) = (\alpha + \beta\cos\theta)^{-1} \sum_{J=m_f}^{\infty} a^{(1)}_J(\alpha,\beta) d^J_{m_f,m_i}(\theta) \quad (3.9)$$

where

$$a^{(1)}_J(\alpha,\beta) = \beta \frac{g^J_{m_f,m_i}}{J(2J-1)} a_{J-1} + \left[\alpha + \beta \frac{m_f m_i}{J(J+1)}\right] a_J + \beta \frac{g^{J+1}_{m_f,m_i}}{(J+1)(2J+3)} a_{J+1}, \quad J = m_f, m_f+1, m_f+2, \ldots \quad (3.10)$$

Equation 3.9 shows that we have, in effect, extracted the factor $(\alpha + \beta\cos\theta)^{-1}$ from the original PWS (eq 3.1). Of course the numerical values of $f_{j_f m_f \leftarrow j_i m_i}(\theta)$ are independent of α and β. Note that we can set $a_J \equiv a^J_{j_f m_f \leftarrow j_i m_i}$ identically equal to zero for nonphysical values of J because they are always multiplied by terms that are zero. By analogy with eq 3.2, we can also introduce an effective scattering matrix element, $S^{J(1)}_{j_f m_f \leftarrow j_i m_i}(\alpha,\beta)$, for the resummed series (eq 3.9)

$$a^{(1)}_J(\alpha,\beta) \equiv a^{J(1)}_{j_f m_f \leftarrow j_i m_i}(\alpha,\beta) = (2J+1)[S^{J(1)}_{j_f m_f \leftarrow j_i m_i}(\alpha,\beta) - \delta_{j_f j_i}\delta_{m_f m_i}] \quad (3.11)$$

Substituting eq 2.4 into eq 3.9 gives us the NF decomposition of the resummed series. We can write

$$f_{j_f m_f \leftarrow j_i m_i}(\theta) = f^{(+)(1)}_{j_f m_f \leftarrow j_i m_i}(\alpha,\beta;\theta) + f^{(-)(1)}_{j_f m_f \leftarrow j_i m_i}(\alpha,\beta;\theta) \quad (3.12)$$

where

$$2ik_{j_i} f^{(\pm)(1)}_{j_f m_f \leftarrow j_i m_i}(\alpha,\beta;\theta) = (\alpha + \beta\cos\theta)^{-1} \sum_{J=m_f}^{\infty} a^{(1)}_J(\alpha,\beta) d^{J(\pm)}_{m_f,m_i}(\theta) \quad (3.13)$$

Note that the N and F subamplitudes (eq 3.13) depend on α and β, whereas their sum (eq 3.12) does not. Inspection of eqs 2.5 and 3.13 reveals that the dependence on α and β comes from the series

$$(\alpha + \beta\cos\theta)^{-1} \sum_{J=m_f}^{\infty} a^{(1)}_J(\alpha,\beta) e^J_{m_f,m_i}(\theta)$$

The state-to-state N and F resummed angular distributions are given by

$$I^{(\pm)(1)}_{j_f m_f \leftarrow j_i m_i}(\alpha,\beta;\theta) = |f^{(\pm)(1)}_{j_f m_f \leftarrow j_i m_i}(\alpha,\beta;\theta)|^2 \quad (3.14)$$

Special Case. As a check on the above analysis, we consider the special case $m_f = m_i = 0$ and $\alpha = 1$, $\beta = -1$. With the help of the results

$$g^J_{0,0} = J^2, \quad g^{J+1}_{0,0} = (J+1)^2, \quad d^J_{0,0}(\theta) = P_J(\cos\theta)$$

eqs 3.9 and 3.10 simplify to

$$2ik_{j_i} f_{j_f 0 \leftarrow j_i 0}(\theta) = (1 - \cos\theta)^{-1} \sum_{J=0}^{\infty} a^{(1)}_J(1,-1) P_J(\cos\theta) \quad (3.15)$$

where

$$a^{(1)}_J(1,-1) = -\frac{J}{2J-1} a_{J-1} + a_J - \frac{(J+1)}{2J+3} a_{J+1}, \quad J = 0, 1, 2, \ldots \quad (3.16)$$

[Nota bene, for $J = 0$, the limit $J \rightarrow 0$ has to be taken in eq 3.10]. Equations 3.15 and 3.16 agree with eqs A.4 and A.5 of

ref 23, i.e., the present formalism contains as a special case the resummation method of Yennie et al.[32] for a Legendre PWS.

4. Calculations

This section describes the potential energy function used for the Ar−HF collision system and the coupled-channel (CC) computations of the angular scattering.

(a) Intermolecular Potential Energy Function. We used the Hutson H6(4,3,2) potential function[6] to describe the interaction of Ar with HF($v = 0$), where v is the vibrational quantum number. This potential, which has 22 adjustable parameters, has been deduced from high-resolution microwave, far-infrared and infrared spectroscopic data. Subsequently, it has been found to perform well[5,7−9] for rotationally inelastic collisions, which sample the repulsive wall of the potential. The H6 potential has a well depth of 220.2 cm^{-1} in the collinear Ar−HF configuration and a secondary minimum at the collinear Ar−FH geometry of depth 107.5 cm^{-1}. A FORTRAN 77 version of the H6 potential was kindly supplied to us by Professor J. M. Hutson.

(b) Scattering Calculations. The CC scattering computations were carried out using the computer code MOLSCAT (version 14).[33] HF was assumed to be a rigid rotator with a bond distance of $r_0 = 0.09326$ nm and a rotational constant of $B_0 = 20.25$ cm^{-1}. The reduced mass of Ar−HF is $\mu = 13.33$ u.We performed calculations at eight energies, E, measured relative to the ground rotational state of HF, corresponding to the wavenumbers E/hc = 350(100)950 and 1089 cm^{-1}. (The notation w = x(y)z means increment w in steps of y starting from w = x and finishing at w = z.) This enabled us to examine trends in the scattering results as a function of E. The lowest wavenumber, $E/hc = 350$ cm^{-1}, is that used in the dopplerimetry experiment of Chapman et al.,[5] while E/hc = 1089 cm^{-1} corresponds to the energy of the Rawluk et al.[4] differential cross section measurements.

The basis set comprised rotational states of HF(j), with j = 0, 1, 2, ..., j_{max}, where $j_{max} = 9$ at the lowest E and $j_{max} = 11$ at the highest E. These values correspond to four open and six closed states at $E/hc = 350$ cm^{-1} and seven open and five closed states at E/hc = 1089 cm^{-1}. The CC calculations were performed from $J = 0$ to J_{max} with $\Delta J = 1$ where $J_{max} = 187$ at the lowest E and $J_{max} = 416$ at the highest E, i.e., J = 0(1)J_{max}. The diabatic modified log derivative method of Manolopoulos[34] was used to solve the coupled differential equations.

The scattering matrix elements produced by MOLSCAT are in a space-fixed (SF) reference frame, being labeled by J,j_i,j_f and by l_i, l_f, the initial and final orbital angular momentum quantum numbers, respectively. The helicity S matrix elements are obtained from the SF ones using[20,27,28]

$$S^J_{j_f m_f \leftarrow j_i m_i} = \sum_{l_f=|J-j_f|}^{J+j_f} \sum_{l_i=|J-j_i|}^{J+j_i} i^{l_i - l_f} \langle j_f m_f, J - m_f | l_f 0 \rangle S^J_{j_i l_f \leftarrow j_i l_i} \langle j_i m_i, J - m_i | l_i 0 \rangle \quad (4.1)$$

where $\langle j_1 m_1, j_2 m_2 | j m \rangle$ is a Clebsch−Gordon coefficient with $m = m_1 + m_2$. Note in eq 4.1, m_i lies in the range $-\min(j_i, J)$ to $+\min(j_i, J)$ and similarly for m_f.

From $S^J_{j_f m_f \leftarrow j_i m_i}$, the CC, NF, and resummed NF state-to-state differential cross sections were calculated as described in sections 2 and 3. In addition, we also computed degeneracy-averaged cross sections e.g., for the CC case

$$I_{j_f \leftarrow j_i}(\theta) = (2j_i + 1)^{-1} \sum_{m_f=-j_f}^{j_f} \sum_{m_i=-j_i}^{j_i} I_{j_f m_f \leftarrow j_i m_i}(\theta) \quad (4.2)$$

and similarly for the N and F angular distributions.

For the special case $m_f = m_i = 0$, the $J = 0$ partial wave is problematic for the NF analysis because $d^0_{0,0}(\theta) = P_0(\cos\theta) = 1$ is independent of θ, whereas the $d^{0(\pm)}_{0,0}(\theta)$ are θ dependent. Following earlier work,[17,20,25] we omitted the $J = 0$ partial wave from eqs 2.11 and 3.13 when $m_f = m_i = 0$.

5. Results and Discussion

5.1. Introduction. This section presents our results for the NF and full PWS angular distributions. Since the aim of the NF method is to provide physical insight into the origin of structure in differential cross sections, we will display our NF and PWS cross sections graphically. We do not show angular distributions at all eight collision energies; rather, we have selected results which illustrate the main trends and which are relevant to the experiments.[4,5]

As discussed in refs 17, 22, and 23 for Legendre PWS, the NF decomposition (eq 2.4) is not unique—there are an infinity of possible decompositions. Thus, there is no guarantee that the subamplitudes (eq 2.11) will provide useful results in the sense of being physically meaningful, even though by construction, the NF decomposition is exact. An example of a useful NF decomposition is when $I^{(+)}_{j_f m_f \leftarrow j_i m_i}(\theta)$ and/or $I^{(-)}_{j_f m_f \leftarrow j_i m_i}(\theta)$ contain less (or comparable) structure than does $I_{j_f m_f \leftarrow j_i m_i}(\theta)$. In addition, the magnitudes of the NF angular distributions should be similar (or smaller) than the magnitude of $I_{j_f m_f \leftarrow j_i m_i}(\theta)$. Conversely, a NF decomposition is not useful when the NF angular distributions are more structured than is $I_{j_f m_f \leftarrow j_i m_i}(\theta)$. Again, a NF decomposition is not useful when $I^{(\pm)}_{j_f m_f \leftarrow j_i m_i}(\theta) \gg I_{j_f m_f \leftarrow j_i m_i}(\theta)$. Examples of successful and (occasionally) unsuccessful NF analyses will be seen in the graphs presented below.

5.2. Nearside−Farside Results. Figure 1 shows the PWS and NF differential cross sections at $E/hc = 350$, 750, and 1089 cm^{-1} for the rotationally elastic transition (0, 0) → (0, 0), where we will label the transitions (j_i, m_i) → (j_f, m_f) from now on. At $E/hc = 350$ cm^{-1}, we can see in the PWS cross section for $\theta \lesssim 90°$ a characteristic rainbow scattering pattern plus high-frequency oscillations. The F angular distribution possesses a broad Airy-like oscillation with a maximum at $\theta \approx 30°$ and a supernumerary rainbow at smaller θ. This F scattering arises from the attractive part of the potential. In contrast for $\theta \gtrsim 90°$, the N cross section dominates the angular distribution, which arises from scattering by the repulsive core of the potential. Figure 1 also clearly shows that the high frequency (diffraction) oscillations for $\theta \lesssim 90°$ are the result of interference between the N and F subamplitudes. Indeed a simple NF model[16] gives for the oscillation period

$$\Delta\theta \approx \pi/k_{j_i} R \quad (5.1)$$

where R is the radius of the potential core. A fit to the Hutson potential at $E/hc = 350$ cm^{-1} yields $R \approx 0.3$ nm, and eq 5.1 then gives $\Delta\theta \approx 0.063$ rad $\approx 3.6°$, in agreement with Figure 1. Evidently the (0, 0) → (0, 0) angular scattering at $E/hc = 350$ cm^{-1} is analogous to that for rainbow scattering from a spherically symmetric potential (see section VIC of ref 17 for a detailed NF analysis of this case).

As E/hc increases through 750 to 1089 cm^{-1}, Figure 1 shows that the F cross section loses its rainbow oscillation and becomes monotonic. At the same time, the N angular distribution acquires a broad maximum, which is located at $\theta \approx 60°$ for $E/hc = 1089$ cm^{-1}. For this wavenumber, Figure 1 shows that the N and F angular distributions cross at $\theta \approx 20°$ and the corresponding subamplitudes interfere to produce high-frequency oscillations in the PWS differential cross section. Equation 5.1 gives for

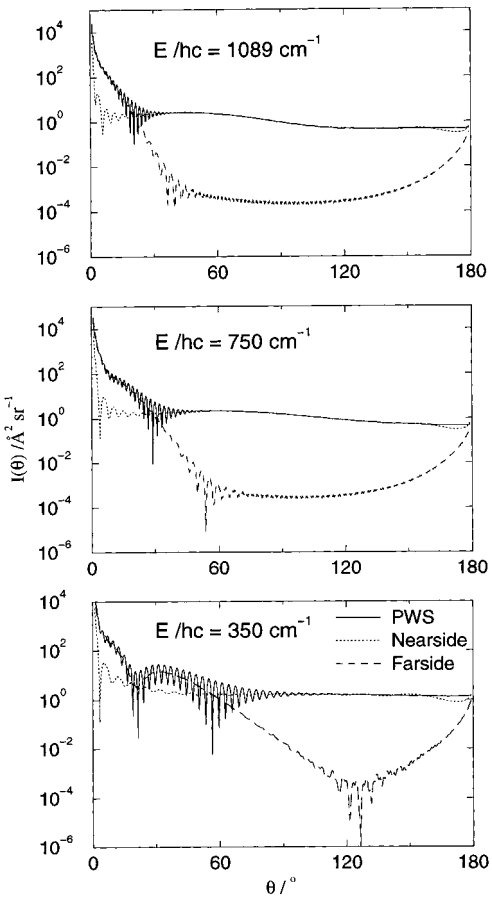

Figure 1. Differential cross sections, $I(\theta)$ versus θ, for the elastic (0,0) → (0,0) transition in the Ar + HF(j_i, m_i) → Ar + HF(j_f, m_f) collision system at E/hc = 350, 750, and 1089 cm^{-1}. Solid line: angular distribution (PWS) calculated by summation of the partial wave series (eq 2.1). Dotted line: nearside angular distribution calculated by summation of the partial wave series (eq 2.11). Dashed line: farside angular distribution calculated by summation of the partial wave series (eq 2.11).

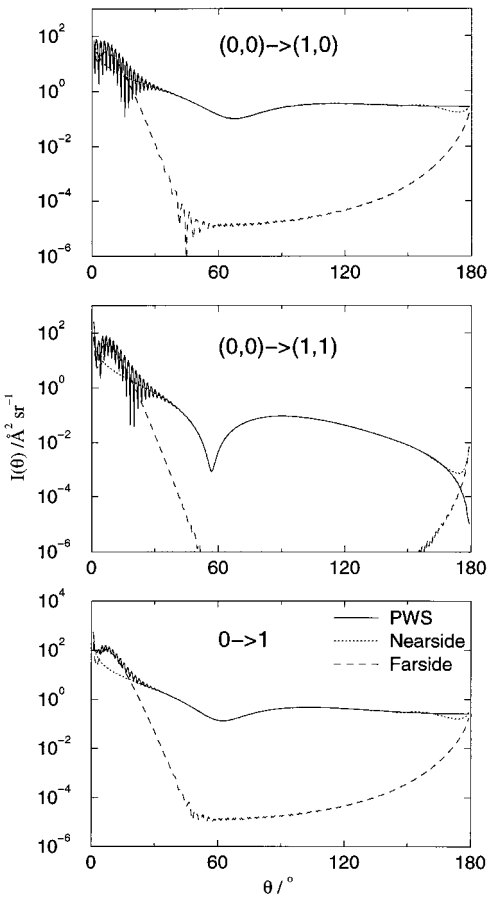

Figure 2. Same as Figure 1 except for E/hc = 1089 cm^{-1} and the transitions (0,0) → (1,0), (0,0) → (1,1). Also shown is $I(\theta)$ versus θ for the degeneracy-averaged transition $j_i = 0 \rightarrow j_f = 1$.

the period $\Delta\theta \approx 0.036$ rad $\approx 2.0°$ in agreement with Figure 1. If these high-frequency oscillations are averaged over, there results a broad shoulder in the angular scattering from $\theta \approx 20°-90°$. The NF analysis shows this shoulder receives contributions from both the N and F subamplitudes at $\theta \approx 20°$, becoming N dominated as θ increases. This NF analysis is consistent with the conclusion of refs 7−9, that the shoulder corresponds to collisions sampling both the repulsive and attractive parts of the potential. The shoulder has been observed in the molecular beam experiments of Rawluk et al.,[4] which however include a contribution from HF($j_i = 1$).

Figures 2−4 show the PWS and NF angular distributions for the (0, 0) → (1, 0) and (0, 0) → (1, 1) transitions, as well as for the degeneracy averaged $j_i = 0 \rightarrow j_f = 1$ transition at E/hc = 1089, 750, and 350 cm^{-1}, respectively. Note that the cross sections for the (0, 0) → (1, −1) transition are equal to those for the (0, 0) → (1, 1) transition because of the identity[20]

$$I_{j_f-m_f\leftarrow j_i0}(\theta) = I_{j_fm_f\leftarrow j_i0}(\theta)$$

(and similarly for the NF angular distributions). The most striking features are the minima in the (0, 0) → (1, 0) and the (0, 0) → (1, 1) cross sections at $\theta \approx 60°$ for E/hc = 1089 cm^{-1} which move to $\theta \approx 120°$ for E/hc = 350 cm^{-1}. The same feature is also evident in the degeneracy averaged angular distributions. Figures 2−4 show that the minima are N dominated, i.e., the scattering occurs mainly from the repulsive core of the potential. This is consistent with the two-state semiclassical model of refs 8 and 9, which identifies a minimum in the opacity function and a trajectory deflected by the repulsive part of the potential (but accumulating net zero action), as important for interpreting the minimum in $I_{1\leftarrow 0}(\theta)$ at E/hc = 1089 cm^{-1}.

For θ smaller than the minima, Figures 2−4, exhibit (distorted) potential rainbow scattering and diffraction oscillations similar to that already discussed for the (0, 0) → (0, 0) transition in Figure 1. At $\theta = 0°$ and 180° we have

$$I_{j_fm_f\leftarrow j_i0}(\theta = 0, \pi) = 0 \qquad \text{for} \qquad m_f > 0$$

which follows from the identities

$$d^J_{m_f,0}(0) = \delta_{m_f0} \quad \text{and} \quad d^J_{m_f,0}(\pi) = (-1)^J\delta_{m_f0}$$

[ref 29, pp 58, 59, eqs. 4.1.17, 4.1.23, and 4.2.1]. In contrast, the $d^{(\pm)}_{m_f,0}(\theta)$ diverge as $\theta \rightarrow 0, \pi$. This behavior can be seen most clearly for the (0, 0) → (1, 1) transition in Figures 2−4 for the angular range $\theta \approx 170°-180°$. It provides an example of the NF decomposition failing to provide a physically useful interpretation of the scattering because $I^{(\pm)}_{11\leftarrow 00}(\theta) \gg I_{11\leftarrow 00}(\theta)$ in this angular range. The divergence of the N and F cross sections can be removed by using a restricted NF decomposition[20,25] rather than the present unrestricted NF theory. However, since the angular regions in Figures 2−4 are small where the unrestricted theory fails, we have not used the more sophisticated restricted theory in this paper.

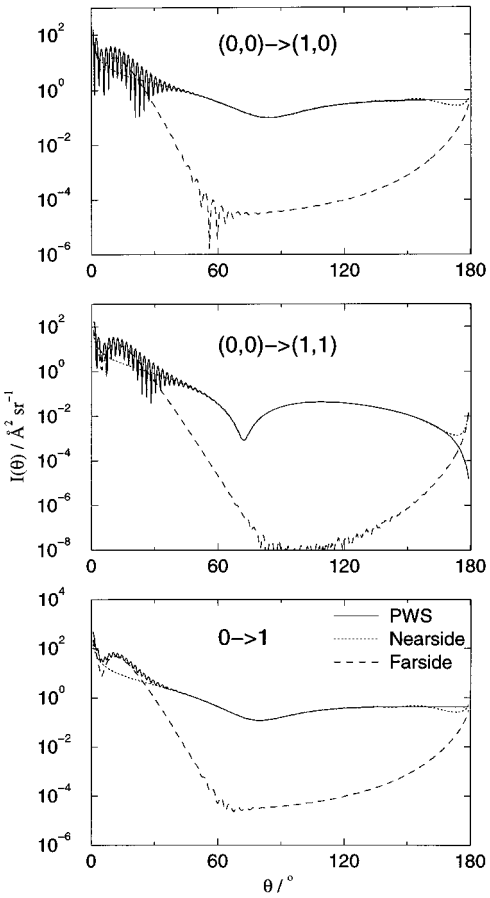

Figure 3. Same as Figure 1 except for $E/hc = 750$ cm^{-1} and the transitions (0,0) → (1,0), (0,0) → (1,1). Also shown is $I(\theta)$ versus θ for the degeneracy-averaged transition $j_i = 0 \rightarrow j_f = 1$.

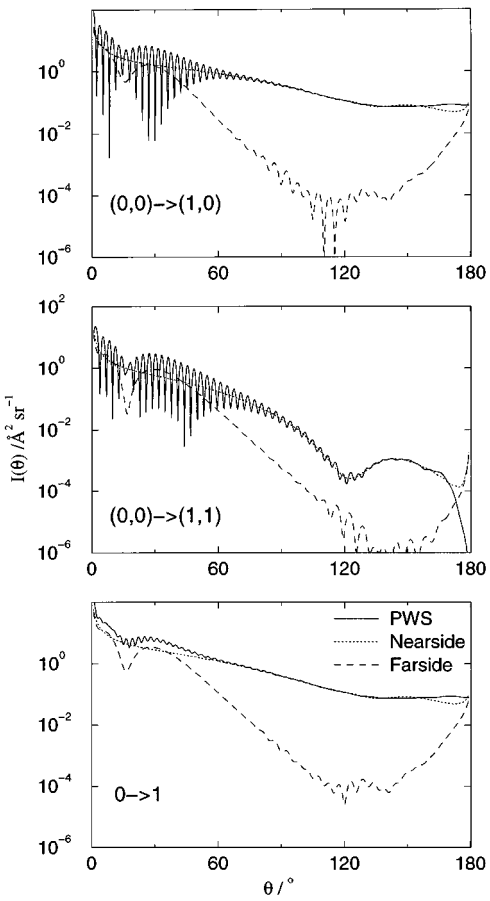

Figure 4. Same as Figure 1 except for $E/hc = 350$ cm^{-1} and the transitions (0,0) → (1,0), (0,0) → (1,1). Also shown is $I(\theta)$ versus θ for the degeneracy-averaged transition $j_i = 0 \rightarrow j_f = 1$.

Figure 5 shows PWS and NF angular distributions at $E/hc = 550$ cm^{-1} for the transitions (0, 0) → (2, m_f) with $m_f = 0, 1, 2$ (the degeneracy averaged cross section for $j_i = 0 \rightarrow j_f = 2$ is also displayed). The results are generally similar to those discussed above. Thus, the large angle scattering is N dominated with diffraction effects at smaller θ arising from interference between the N and F subamplitudes. We do not see the characteristic potential rainbow structure in the F cross section any more. Figure 6 shows that similar comments apply at $E/hc = 1089$ cm^{-1} to the transitions (0, 0) → (3, m_f) with $m_f = 0, 1, 2, 3$ and the degeneracy averaged $j_i = 0 \rightarrow j_f = 3$ cross section.

All the angular distributions discussed above have been for an atom−heteronuclear molecule collision. However, we note that unusual minima beyond the rainbow region can also occur for atom−homonuclear molecule collisions. For examples, see Figures 5 and 6 of ref 35, which show degeneracy averaged angular distributions for the $j_i = 0 \rightarrow j_f = 0$ and $j_i = 0 \rightarrow j_f = 2$ transitions in the Ar + N_2 collision system as well as refs 20 and 25.

5.3. Nearside−Farside Results Using Resummed Partial Wave Series. All of the NF cross sections discussed so far in Figures 1−6 have used the unresummed NF theory of section 2. We next consider two examples that illustrate the resummed NF theory developed in section 3.

Figure 7 (top part) shows PWS and NF angular distributions in the range $\theta = 0°-60°$ for the (0, 0) → (2, 0) transition at $E/hc = 450$ cm^{-1}. The diffraction oscillations in the PWS cross section with period $\Delta\theta \approx 3°$ are clearly visible. The N and F cross sections exhibit a simpler structure than does the PWS angular distribution, which provides a physically meaningful explanation of the high-frequency oscillations as a NF interference effect. Nevertheless the N cross section, and to a lesser extent the F cross section, also possess small oscillations with a period of $\Delta\theta \approx 6°$. This raises the question: Are these oscillations an artefact of the NF decomposition (eq 2.10) or are they physically meaningful, as is the case for the Airy-like undulations in the elastic F cross section of Figure 1 at $E/hc = 350$ cm^{-1}?

In refs 22 and 23, Hollifield and one of us applied the resummation method of Yennie et al.[32] to a Legendre PWS, which was then followed by a NF decomposition. (Nota bene: in the present notation, that work[22,23] corresponds to $\alpha = 1$, $\beta = -1$, and $m_f = m_i = 0$, see also ref 36). An application was made to elastic scattering in strongly absorptive collisions. It was demonstrated that a resummation significantly increases the angular range over which the NF decomposition provides a physically meaningful interpretation of interference effects in the differential cross sections.[22,23]

Figure 7 (middle part) shows the N and F cross sections that result from using $\alpha = 1$, $\beta = -1$ in the resummed NF decomposition, eq 3.13 and 3.14. It can be seen that the N and F angular distributions possess pronounced oscillations, which increase in amplitude as θ decreases. Thus, unlike refs 22 and 23, the NF decomposition (eq 3.13) with $\alpha = 1$, $\beta = -1$ has not provided us with an (improved) physically meaningful interpretation of the diffraction oscillations in Figure 7; in fact, it is much worse than the unresummed decomposition (eq 2.10).

Figure 7 (lower part) also shows the N and F angular distributions obtained using $\alpha = 1$, $\beta = 0.9$. The N and F curves are now oscillation free and provide a clearer physical inter-

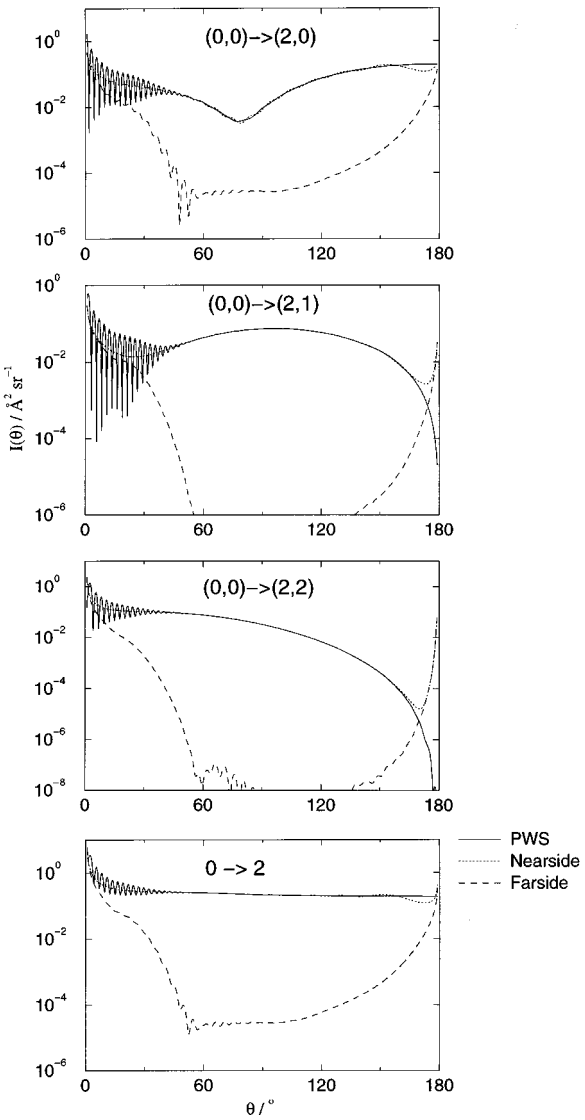

Figure 5. Same as Figure 1 except for $E/hc = 550$ cm^{-1} and the transitions (0,0) → (2,0), (0,0) → (2,1), (0,0) → (2,2). Also shown is $I(\theta)$ versus θ for the degeneracy-averaged transition $j_i = 0 \rightarrow j_f = 2$.

pretation of the diffraction oscillations than does the unresummed NF analysis. To understand the results in Figure 7, we show in Figure 8 for $E/hc = 450$ cm^{-1} graphs of the following quantities versus J

$$\text{Re } S^{J}_{20\leftarrow 00}\text{ , Im } S^{J}_{20\leftarrow 00}$$

$$\text{Re } S^{J(1)}_{20\leftarrow 00}(1,-1)\text{, Im } S^{J(1)}_{20\leftarrow 00}(1,-1)$$

$$\text{Re } S^{J(1)}_{20\leftarrow 00}(1,0.9)\text{, Im } S^{J(1)}_{20\leftarrow 00}(1,0.9)$$

where $S^{J}_{j_f m_f \leftarrow j_i m_i}$ and $S^{J(1)}_{j_f m_f \leftarrow j_i m_i}(\alpha,\beta)$ are given by eqs 2.1 and 3.11, respectively. Figure 8 (middle and lower parts) shows that the values of $S^{J(1)}_{20\leftarrow 00}(\alpha,\beta)$ for $\alpha = 1$, $\beta = -1$ at small J are enhanced relative to $S^{J}_{20\leftarrow 00}$ but diminished for $\alpha = 1$, $\beta = 0.9$. In particular, when $\alpha = 1$, $\beta = 0.9$, the effect of the resummation has been to move the largest contributions in the sum (eq 3.13) to higher values of J. As discussed in refs 22 and 23 for Legendre PWS, this effect favors a physically meaningful NF analysis of structure in a differential cross section, because the $d^{J(\pm)}_{m_f,m_i}(\theta)$ become travelling angular waves when $J \gg 1$, see eq 2.9.

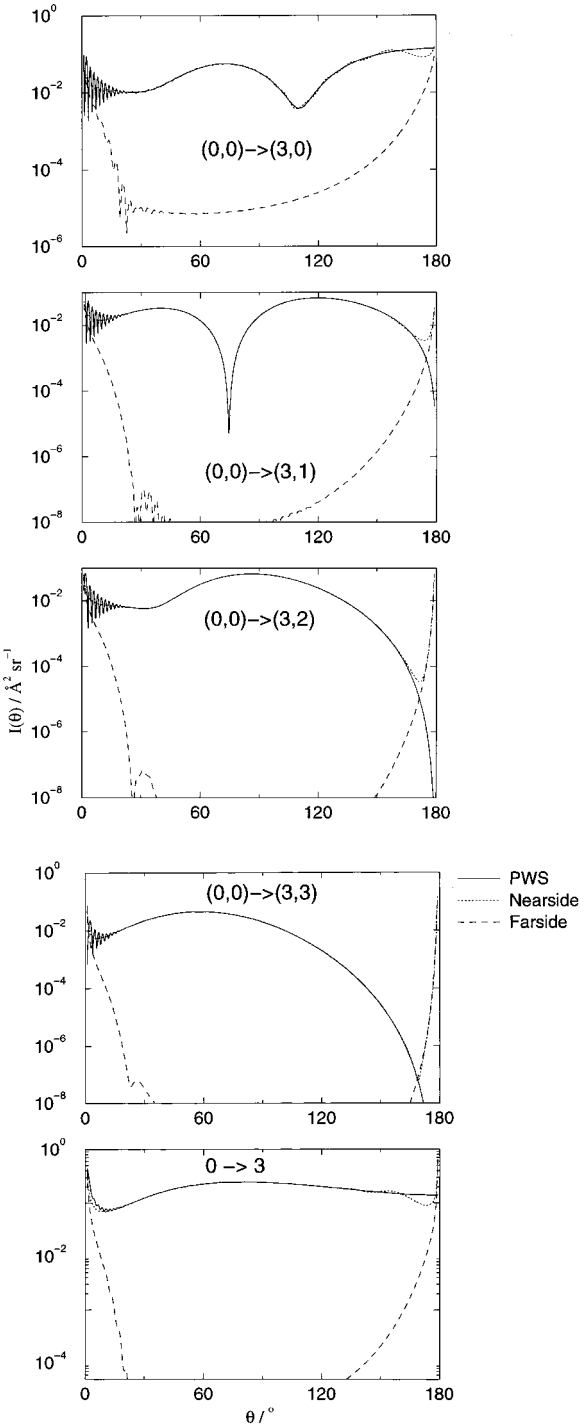

Figure 6. Same as Figure 1 except for $E/hc = 1089$ cm^{-1} and the transitions (0,0) → (3,0), (0,0) → (3,1), (0,0) → (3,2), (0,0) → (3,3). Also shown is $I(\theta)$ versus θ for the degeneracy-averaged transition $j_i = 0 \rightarrow j_f = 3$.

Next we discuss the problem of how to choose values for α and β so that physically meaningful NF decompositions are produced. Comparing eq 3.9 with eq 3.1 shows that we have extracted a factor $(\alpha + \beta\cos\theta)^{-1}$ from the original PWS (3.1). For $\alpha = 1$, $\beta = -1$, the factor $(1 - \cos\theta)^{-1}$ has a large peak in the forward direction with a second-order pole at $\theta = 0°$. However, $I_{20\leftarrow 00}(\theta)$ does not have a large peak in the forward direction, rather there is more scattering into $\theta > 90°$ than into $\theta < 90°$. When $\alpha = 1$, $\beta = 0.9$ on the other hand, the factor $(1 + 0.9\cos\theta)^{-1}$ rises gently to a maximum at $\theta = 180°$. In both cases, the sums in eq 3.9 have to compensate for the behavior

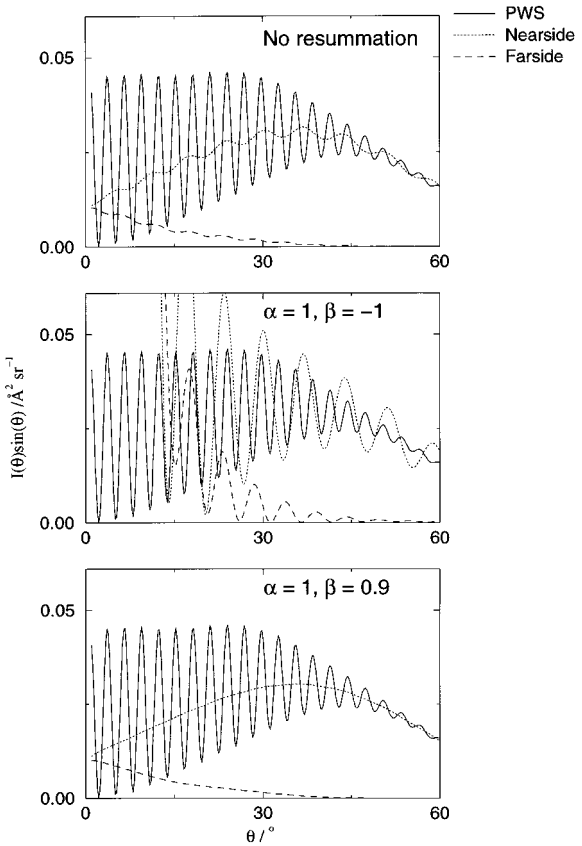

Figure 7. Angular distributions, $I(\theta)$ sin θ versus θ, for $E/hc = 450$ cm^{-1} and the transition (0,0) → (2,0) showing the effect of no resummation, resummation using $\alpha = 1$, $\beta = -1$ and resummation using $\alpha = 1$, $\beta = 0.9$. Solid line: angular distribution (PWS) calculated by summation of the partial waves series (eq 2.1) [or resummed partial wave series (eq 3.9)]. Dotted line: nearside angular distribution calculated by summation of the resummed partial wave series (eq 3.13). Dashed line: farside angular distribution calculated by summation of the resummed partial wave series (eq 3.13).

of $(\alpha + \beta\cos\theta)^{-1}$. Evidently when $(\alpha + \beta\cos\theta)^{-1}$ approximates the shape of $I_{20\leftarrow 00}(\theta)$, the sums in eqs 3.9 and 3.13 are better behaved in producing physically meaningful NF decompositions.

Figure 9 (upper panel) shows PWS and NF angular distributions in the range $\theta = 0° - 60°$ for the (0, 0) → (3, 0) transition at $E/hc = 650$ cm^{-1}. Both the N and F cross sections possess oscillations with a period of $\Delta\theta \approx 5.5°$. In contrast to Figure 7, the F oscillations are the more pronounced. Using $\alpha = 1$, $\beta = -1$ in the resummed series (3.13) yields N and F cross sections in Figure 9 (middle panel) that are much larger than $I_{30\leftarrow 00}(\theta)$ as θ decreases. In addition, the N angular distribution possesses large oscillations. Evidently $\alpha = 1$, $\beta = -1$ has failed once again to provide a physically meaningful interpretation of the high-frequency oscillations in $I_{30\leftarrow 00}(\theta)$. In contrast, Figure 9 (lower panel) shows that $\alpha = 1$, $\beta = 0.9$ produces oscillation-free and physically meaningful N and F cross sections.

Figure 10 displays plots of the real and imaginary part of $S^J_{30\leftarrow 00}$ and $S^{J(1)}_{30\leftarrow 00}(\alpha,\beta)$ versus J. The trends are similar to those in Figure 8. Thus, the lower partial waves have been enhanced relative to $S^J_{30\leftarrow 00}$ for $\alpha = 1$, $\beta = -1$ but diminished for $\alpha = 1$, $\beta = 0.9$.

Our discussion of the results in Figures 7−10, together with those in refs 22 and 23 for resummed Legendre PWS, suggests the following rule of thumb for choosing values of α and β that produce physically meaningful N and F cross sections: *Choose values of* α *and* β *so that* $(\alpha + \beta\cos\theta)^{-1}$ *approximately*

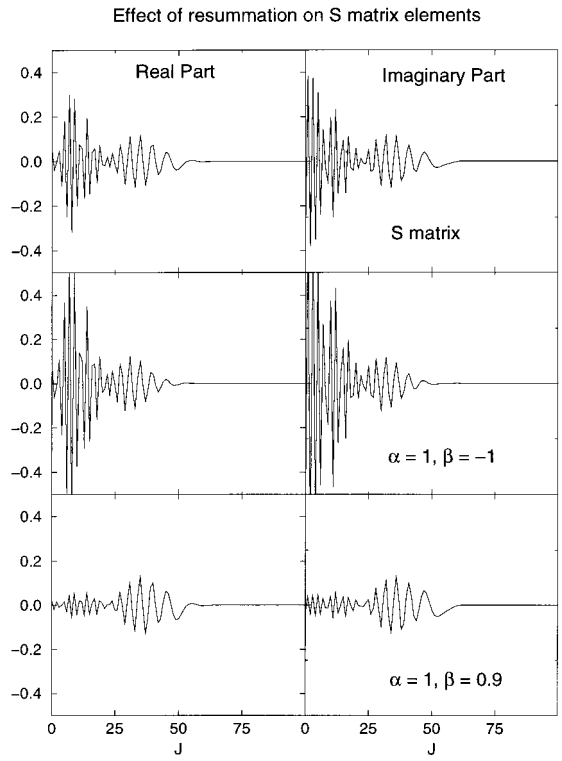

Figure 8. Effect of resummation on the scattering matrix elements for $E/hc = 450$ cm^{-1} and the transition (0,0) → (2,0). Upper part: Re $S^J_{20\leftarrow 00}$ versus J (left) and Im $S^J_{20\leftarrow 00}$ versus J (right). Middle part: Re $S^{J(1)}_{20\leftarrow 00}(\alpha,\beta)$ versus J (left) and Im $S^{J(1)}_{20\leftarrow 00}(\alpha,\beta)$ versus J (right) for $\alpha = 1$, $\beta = -1$. Lower part: Re $S^{J(1)}_{20\leftarrow 00}(\alpha,\beta)$ versus J (left) and Im $S^{J(1)}_{20\leftarrow 00}(\alpha,\beta)$ versus J (right) for $\alpha = 1$, $\beta = 0.9$.

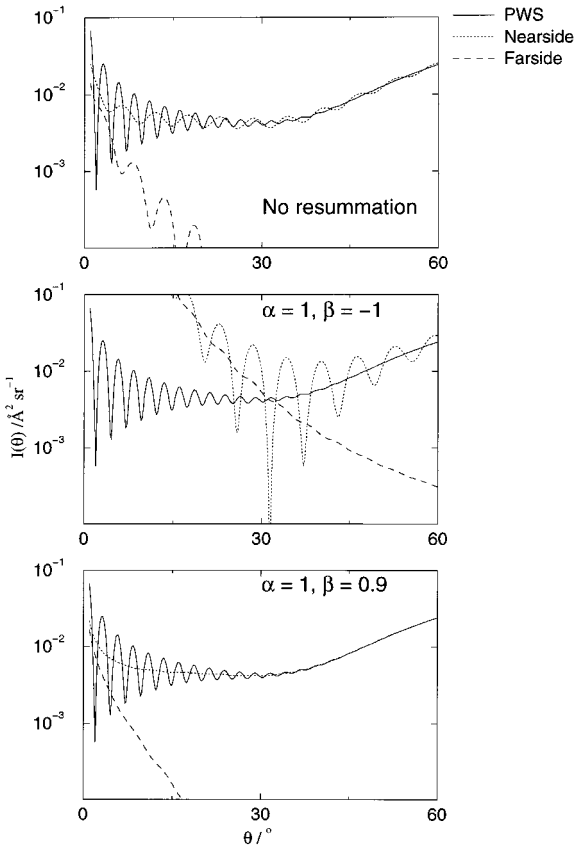

Figure 9. Same as Figure 7 except for $I(\theta)$ versus θ, $E/hc = 650$ cm^{-1} and the transition (0,0) → (3,0).

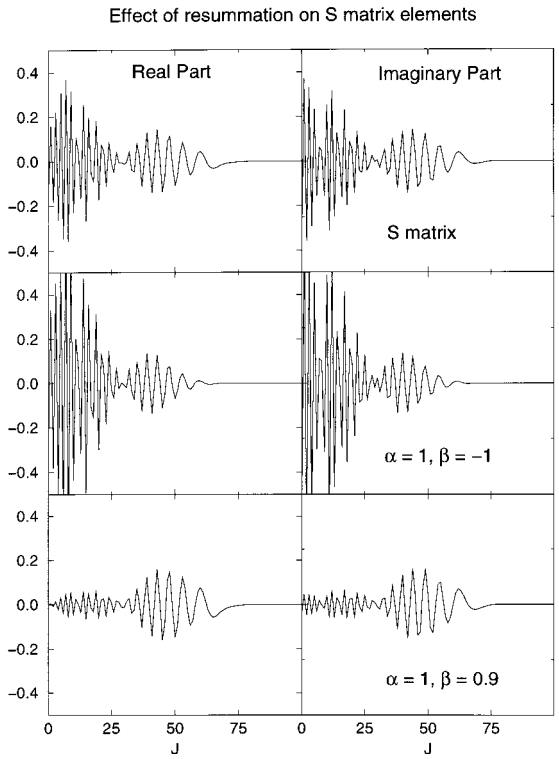

Figure 10. Same as Figure 8 except for $E/hc = 650$ cm^{-1} and the transition (0,0) → (3,0).

mimics the shape of $I_{j_f m_f \leftarrow j_i m_i}(\theta)$ in order to obtain physically meaningful N and F cross sections.

A more precise method to determine values for α and β would be to fit $(\alpha + \beta\cos\theta)^{-1}$ to $I_{j_f m_f \leftarrow j_i m_i}(\theta)$ by, e.g., least squares. In addition, the resummation theory of section 3 could be generalized by extracting the more general factor $(\alpha + \beta\cos\theta + \gamma\cos^2\theta + ...)^{-1}$ from the PWS and seeing if there are an optimal number of terms that yields the best possible NF decomposition.

6. Conclusions

We have carried out accurate coupled-channel quantum calculations of PWS and unrestricted NF differential cross sections for the rotationally inelastic Ar + HF collision system. Our calculations have complemented earlier theoretical work and are also relevant to the experiments of Vohralik et al.,[3] Rawluk et al.,[4] and Chapman et al.[5] The results we presented represent the first application of NF theory to an atom−heteronuclear molecule inelastic collision. We found that the NF decomposition of the scattering amplitude provides a clear physical interpretation of the angular scattering, except sometimes for $\theta \approx 0°$, 180°. We also demonstrated that a resummation of the PWS can improve the usefulness of the NF technique when the N and F cross sections possess small oscillations. The resummation procedure exploits recurrence properties of reduced rotation matrix elements to extract the factor $(\alpha + \beta\cos\theta)^{-1}$ from the PWS. We proposed a rule of thumb for choosing α and β so as to produce physically meaningful NF decompositions.

Acknowledgment. We thank Prof. J. M. Hutson (University of Durham, U.K.) for advice concerning MOLSCAT and the intermolecular potential function for ArHF. Support of this research by the Engineering and Physical Sciences Research Council (U.K.) and INTAS (E.U.) is gratefully acknowledged.

Appendix

In section 3, we used properties of the $d^J_{m_f,m_i}(\theta)$ where $J \geq m_f \geq |m_i|$. In particular, we exploited the following recurrence relation to resum the PWS (eq 3.1)

$$d^{J+1}_{m_f,m_i}(\theta) = \frac{(J+1)(2J+1)}{g^{J+1}_{m_f,m_i}}\left[\cos\theta - \frac{m_f m_i}{J(J+1)}\right]d^J_{m_f,m_i}(\theta) - \frac{(J+1)}{J}\frac{g^J_{m_f,m_i}}{g^{J+1}_{m_f,m_i}}d^{J-1}_{m_f,m_i}(\theta) \quad \text{(A.1)}$$

where

$$g^{J+p}_{m_f,m_i} = [(J - m_f + p)(J + m_f + p)(J - m_i + p) \times (J + m_i + p)]^{1/2} \qquad p = 0,1 \quad \text{(A.2)}$$

The recurrence (eq A.1) connects terms in $J-1$, J, $J+1$ and is valid for $J = m_f + 1$, $m_f + 2$, ... The purpose of this Appendix is to show that eq A.1 is also valid for $J = m_f$.

First we note that $d^{J-1}_{m_f,m_i}(\theta)$ is nonphysical for $J = m_f$; we can set it identically to zero, i.e., $d^{m_f-1}_{m_f,m_i}(\theta) \equiv 0$. In addition, eq A.2 shows that $g^{m_f}_{m_f,m_i} = 0$. Thus, for $J = m_f$, the right-hand side of eq A.1 becomes

$$\frac{(m_f+1)(2m_f+1)}{g^{m_f+1}_{m_f,m_i}}\left[\cos\theta - \frac{m_i}{m_f+1}\right]d^{m_f}_{m_f,m_i}(\theta) \quad \text{(A.3)}$$

The second step is to verify that expression A.3 is equal to the left-hand side of eq A.1 for $J = m_f$, i.e., equal to $d^{m_f+1}_{m_f,m_i}(\theta)$. To do this, we obtain explicit formulas for $d^{m_f}_{m_f,m_i}(\theta)$ and $d^{m_f+1}_{m_f,m_i}(\theta)$ by relating $d^J_{m_f,m_i}(\theta)$ to a Jacobi polynomial $P_n^{(\alpha,\beta)}(\cos\theta)$ of degree n with parameters α and β. From ref 29, p 58, eq 4.1.23, the required relation is

$$d^J_{m_f,m_i}(\theta) = N^J_{m_f,m_i}[\sin(\theta/2)]^\alpha[\cos(\theta/2)]^\beta P^{(\alpha,\beta)}_{J-m_f}(\cos\theta)$$
$$\alpha = m_f - m_i, \quad \beta = m_f + m_i \quad \text{(A.4)}$$

where

$$N^J_{m_f,m_i} = \left[\frac{(J+m_f)!(J-m_f)!}{(J+m_i)!(J-m_i)!}\right]^{1/2}$$

Now $J = m_f$ and $J = m_f + 1$ correspond to $n = 0$ and $n = 1$, respectively. Since

$$P_0^{(\alpha,\beta)}(\cos\theta) = 1$$

and

$$P_1^{(\alpha,\beta)}(\cos\theta) = \frac{1}{2}[(\alpha+\beta+2)\cos\theta + \alpha - \beta]$$

we obtain from eq A.4 the following results

$$d^{m_f}_{m_f,m_i}(\theta) = \left[\frac{(2m_f)!}{(m_f+m_i)!(m_f-m_i)!}\right]^{1/2}\left[\sin\left(\frac{\theta}{2}\right)\right]^{m_f-m_i}\left[\cos\left(\frac{\theta}{2}\right)\right]^{m_f+m_i}$$

and

$$d^{m_f+1}_{m_f,m_i}(\theta) = \left[\frac{(2m_f+1)!}{(m_f+m_i+1)!(m_f-m_i+1)!}\right]^{1/2} [(m_f+1)\cos\theta - m_i]\left[\sin\left(\frac{\theta}{2}\right)\right]^{m_f-m_i}\left[\cos\left(\frac{\theta}{2}\right)\right]^{m_f+m_i}$$

Using these formulas, it can be verified that expression A.3 is equal to $d^{m_f+1}_{m_f,m_i}(\theta)$, i.e., eq A.1, is valid for $J = m_f$ as well as for $J = m_f + 1$, $m_f + 2$, ... For the special case $m_f = m_i = 0$,we have $d^J_{0,0}(\theta) = P_J(\cos\theta)$ and eq A.1 for $J \rightarrow 0$ reduces to $P_1(\cos\theta) = (\cos\theta)P_0(\cos\theta) = \cos\theta$, a well-known result.

References and Notes

(1) Barnes, J. A.; Keil, M.; Kutina, R. E.; Polanyi, J. C. *J. Chem. Phys*. **1980**, *72*, 6306.

(2) Barnes, J. A.; Keil, M.; Kutina, R. E.; Polanyi, J. C. *J. Chem. Phys.* **1982**, *76*, 913.

(3) Vohralik, P. F.; Miller, R. E.; Watts, R. O. *J. Chem. Phys.* **1989**, *90*, 2182.

(4) Rawluk, L. J.; Fan Y. B.; Apelblat Y.; Keil, M. *J. Chem. Phys.* **1991**, *94*, 4205.

(5) Chapman, W. B.; Weida, M. J.; Nesbitt, D. J. *J. Chem. Phys*, **1997**, *106*, 2248.

(6) Hutson, J. M. *J. Chem Phys*, **1992**, *96*, 6752.

(7) Rawluk, L. J.; Keil, M.; Alexander, M. H.; Mayne, H. R.; Barrett, J. J. C. *Chem. Phys. Lett.* **1993**, *202*, 291.

(8) Barrett, J. J. C.; Mayne, H. R.; Keil, M. *J. Chem. Phys.* **1994**, *100*, 304.

(9) Barrett, J. J. C.; Mayne, H. R.; Keil, M.; Rawluk, L. J. *Can. J. Chem*, **1994**, *72*, 985.

(10) Lovejoy, C. M.; Hutson, J. M.; Nesbitt, D. J. *J. Chem. Phys*. **1992**, *97*, 8009.

(11) Chang, H−C.; Tao, F−M.; Klemperer, W.; Healey, C.; Hutson, J. M. *J. Chem. Phys.* **1993**, *99*, 9337.

(12) Green, S.; Hutson, J. M. *J. Chem. Phys.* **1994**, *100*, 891.

(13) Van Duijn, E. J.; Nokhai, R. N.; Hermans, L. J. F. *J. Chem. Phys*. **1996**, *105*, 6375.

(14) Connor, J. N. L.; McCabe, P.; Sokolovski, D.; Schatz, G. C. *Chem. Phys. Lett.* **1993**, *206*, 119.

(15) Sokolovski, D.; Connor, J. N. L.; Schatz, G. C. *Chem. Phys. Lett.* **1995**, *238*, 127.

(16) Sokolovski, D.; Connor, J. N. L.; Schatz, G. C. *J. Chem. Phys.* **1995**, *103*, 5979.

(17) McCabe, P.; Connor, J. N. L. *J. Chem. Phys.* **1996**, *104*, 2297. In the equation below eq 4.6 for "(4) " read "(4.7)".

(18) Sokolovski, D.; Connor, J. N. L.; Schatz, G. C. *Chem. Phys*. **1996**, *207*, 461. In the caption to Table 3, for "listed as" read "listed are" and in Table 4, for "±1.4(−1)" read "±0.1(−1)".

(19) Wimp, J.; McCabe, P.; Connor, J. N. L. *J. Comput. Appl. Math*. **1997**, *82*, 447. In eq 2.4, for "$P_n^{\alpha,\beta}(x)$" read "$P_n^{(\alpha,\beta)}(x)$" and for "$x \notin (-1,1)$" read "$x \in (-1, 1)$".

(20) McCabe, P.; Connor, J. N. L.; Sokolovski, D. *J. Chem. Phys*. **1998**, *108*, 569.

(21) Sokolovski, D.; Connor, J. N. L. *Chem. Phys. Lett*. **1999**, *305*, 238. In eq 9, for "$(\bar{J} - \bar{\Omega}^2)$" read "$(\bar{J}^2 - \bar{\Omega}^2)$" and in the heading of section 2.4, for "$u^J_{m_f,m_i}(\theta)$for" read "for $u^J_{m_f,m_i}(\theta)$".

(22) Hollifield, J. J.; Connor, J. N. L. *Phys. Rev.* A **1999**, *59*, 1694.

(23) Hollifield, J. J.; Connor, J. N. L. *Mol. Phys*. **1999**, *97*, 293.

(24) Dobbyn, A. J.; McCabe, P.; Connor, J. N. L.; Castillo, J. F. *Phys. Chem. Chem. Phys*. **1999**, *1*, 1115.

(25) McCabe, P.; Connor, J. N. L.; Sokolovski, D. *J. Chem. Phys*. **2001**. Accepted for publication.

(26) Connor, J. N. L. *J. Chem. Soc., Faraday Trans.* **1990**, *86*, 1627. In eq 33, for "$\lambda_n(\lambda)$" read "$\lambda_n(\gamma)$".

(27) Jacob, M.; Wick, G. C. *Ann. Phys.* (N. Y.), **1959**, *7*, 404. Goldberger, M. L.; Watson, K. M. *Collision Theory*; Wiley: New York, 1967; Appendix E.

(28) Balint-Kurti, G. G. In *International Review of Science, Physical Chemistry, Series Two, Vol. 1, Theoretical Chemistry*; Buckingham, A, D., Coulson, C. A., Eds.; Butterworths: London, 1975; Chapter 9, pp 283−326.

(29) Edmonds, A. R. *Angular Momentum in Quantum Mechanics*, 2nd ed.; Princeton University: Princeton, 1974 (third printing with corrections).

(30) We follow ref 29, p 22 in calling eqs 2.13 and 2.14 Ferrers' definitions of $P_J^m(x)$ and $Q_J^m(x)$, even though the Reverend N. M. Ferrers in his monograph, *An Elementary Treatise on Spherical Harmonics and Subjects Connected with Them*; MacMillan: London, 1877, only discussed in detail $P_J^m(x)$, which he denoted $T_J^{(m)}(x)$.

(31) Lai, S.-T.; Chiu, Y.-N. *J. Math. Phys.* **1989**, *30*, 844.

(32) Yennie, D. R.; Ravenhall, D. G.; Wilson, R. N. *Phys. Rev*. **1954**, *95*, 500.

(33) Hutson, J. M.; Green, S. MOLSCAT computer code, version 14, 1994, distributed by Collaborative Computational Project No. 6 of the Engineering and Physical Sciences Research Council, U.K.

(34) Manolopoulos, D. E. *J. Chem. Phys.* **1986**, *85*, 6425.

(35) Connor, J. N. L.; Sun, H.; Hutson, J. M. *J. Chem. Soc., Faraday Trans.* **1990**, *86*, 1649.

(36) Wimp, J. *Numer. Algorithms*, **1999**, *21*, 377.